Production of strange particles at LHC from the ALICE experiment

Barnaby Howells
Project Partner: Thomas Ferguson
Supervisors: Prof. D. Evans and Dr R. Lietava

Y4 Project Preliminary Report
December 2023

Abstract

The ALICE (A Large Ion Collider Experiment) collaboration at the Large Hadron Collider (LHC) was developed to study high energy physics through the collisions of heavy ions at ultra-relativistic speeds. In doing so, ALICE creates the extreme energy densities required for a new, strongly-interacting phase of matter called Quark Gluon Plasma (QGP) to form. Due to its short lifetime, QGP is not directly observable, therefore study of this phenomenon is conducted by analysing certain signatures, including the enhanced production of strange hadrons in the presence of QGP. This project will focus on analysis of the singly strange Λ baryon and K^0_S meson, collectively referred to as V^0s, using data obtained from ALICE Run 3. This preliminary report outlines the methods used to perform event selection cuts and presents an outline for the remainder of the project and intended timescales.

1 Background

Quantum Chromodynamics (QCD) is the theoretical framework that explains the dynamics of the strong force, and the interactions among quarks and gluons. Quarks come in six different "flavours", and each one carries one of the three fundamental colour charges of red, green and blue. Similarly, anti-quarks also carry anti-colour charges. Gluons, on the other hand, carry combinations of colour and anti-colour[1]. Gluons mediate the strong force between quarks, and their ability to carry colour charge allows them to interact with other quarks and gluons. This colour charge creates an increasing potential energy between quarks and gluons as they attempt to separate, making it energetically favourable for new quark-antiquark pairs to form spontaneously[2], preventing the isolation of individual colour-charged particles. This phenomenon is known as confinement.

However, at the energy densities created during collisions at the LHC, the binding forces are overcome, leading to the liberation of quarks and gluons in a process known as deconfinement, the result of which is the formation of QGP[3]. Several QGP signatures have been proposed, as means to infer its properties experimentally. One such signal is the idea of strangeness enhancement, where strange particles are produced at higher rates in the presence of a QGP state. This is due to the absence of hadronic binding in QGP, meaning quarks have a bare mass, rather than the effective mass imparted by the binding process in ordinary matter. As a result, the thermal production of strange quark-antiquark pairs is more likely, resulting in the enhanced production of strange hadrons, something which can be investigated analytically. In current cosmological models, it is believed that up to a few microseconds after the big bang (between 10^{-12} and 10^{-6} seconds), the universe was in a QGP state[4]. The ongoing ALICE experiment is motivated by a desire to better understand QGP and therefore gain insight into the early universe's evolution.

2 ALICE Detector

The ALICE detector is the primary one at the LHC optimised to study QGP. In heavy-ion collisions observed by ALICE, the decay products traverse successive layers from the collision point outwards. These layers include tracking detectors, an electromagnetic and hadronic calorimeter and finally a muon system[5]. An external magnetic field is supplied in order to bend the paths of charged particles, allowing for their charge and momentum to be determined. In total, the detector extends 26m in length and 16m in height and width and is capable of recording Pb-Pb collisions at an interaction rate of up to 50kHz.

A key property of particles produced during collisions is their transverse momentum, p_t, defined as the component of a particle's momentum perpendicular to the beam, $p_t = \sqrt{p_x^2 + p_y^2}$, assuming the beam propagates along the z axis. Another concept used to describe the motion of particles in high-energy physics is pseudo-rapidity, η, defined as[6]:

$$\eta = \frac{1}{2} \ln \left(\frac{|\vec{\mathbf{p}}| + p_z}{|\vec{\mathbf{p}}| - p_z} \right) = - \ln \left[\tan \left(\frac{\theta}{2} \right) \right] \tag{1}$$

Where θ is the angle between the particle three-momentum and the positive direction of the beam axis. By definition, $\eta = 0$ for particles travelling precisely perpendicular to the beamline, and approaches infinity as θ tends towards zero. Note, pseudo-rapidity is defined solely based on the angle of the particle's motion relative to the beamline and not on other quantities, such as its energy. This makes it particularly useful in experiments where the precise determination of a particle's energy may be challenging compared to measuring its trajectory.

The subdetectors that comprise ALICE can be separated into three categories: the central barrel, forward detectors and muon arm. The central barrel extends radially outwards from the beamline, in the central pseudo-rapidity range, and houses the main detectors used for particle tracking and Particle IDentification (PID). The key components of the central barrel relevant for our analysis are the Inner Tracking System (ITS) and Time Projection Chamber (TPC).

2.1 Inner Tracking System

The ITS is the first detector encountered by mid-rapidity particles produced during collisions, with the innermost detection layer located 22.4mm from the interaction point. It covers the region ($-1.22 < \eta < 1.22$) and extends approximately 0.4m away from the beam pipe[7]. The ITS is tasked with determining the primary and secondary decay vertices with high precision, and to track and identify particles with low transverse momentum that may not reach the outer detectors. The system itself is comprised of seven layers of silicon pixels, which form a cylinder around the beam pipe[8]. The first three layers comprise the inner barrel (IB) of the ITS, designed to capture particles emerging directly from the collision point and facilitate accurate vertexing, while the outer four layers form the outer barrel (OB), improving the efficiency of tracking particles with larger trajectories.

The ITS is a large area silicon tracker based on the Monolithic Active Pixel Sensor (MAPS) technology, which integrates both sensor and readout electronics on the same silicon substrate, allowing for a compact and highly efficient tracking device[9]. A silicon sensor layer serves as the active material that interacts with charged particles passing through. The silicon layer is then segmented into an array of pixels, each capable of registering the charge produced by ionising particles. In total, the ITS features $10m^2$ of active silicon area and nearly 13 billion pixels.

2.2 Time Projection Chamber

The TPC is a crucial component in the ALICE central barrel designed to track charged particles and provide particle identification. It is a $90m^3$ cylinder filled with gas and divided into two regions by an electrode located at the centre of the chamber. The TPC is filled with a mixture of neon, carbon dioxide and nitrogen, the exact composition of which must be optimised based on ion mobility in the volume, material budget and stability of operation[10]. As charged particles traverse through the TPC, they ionise the gas along their path, freeing electrons in the process that drift towards the end plates of the cylinder. The signal generated is amplified by Gas Electron Multipliers (GEM). GEMs work by creating electron avalanches through a series of perforated foil layers, vastly increasing the number of electrons collected. Finally, PID is achieved by measuring the specific energy loss for each particle as it passes through the TPC[11].

3 Data Analysis

3.1 Selection Cuts

As the K^0_S and Λ are electrically neutral, they escape detection by the ALICE tracking detectors. Therefore, the reconstruction of each potential candidate relies on tracing back their decay products, referred to as the candidate's daughters. Applying a set of selection criteria based on the well-known V^0 decay topologies allows the exclusion of certain candidates. For each V^0 candidate, five selection cuts are available: the distance of closest approach (DCA) between the positive and negative daughter track and the Primary Vertex (PV), the DCA between the V^0 daughters themselves, the V^0 decay radius, and the cosine of the V^0 pointing angle.

To illustrate the workflow for each cut, consider K^0_S analysis for the case of the DCA between the negative daughter track and the PV. In this scenario, a candidate is excluded if the daughter track closely approaches the PV during the reconstruction process. This criterion ensures that the daughter track is more likely to have originated from a weak decay rather than the initial collision. In this case, the default cut is 0.0, meaning no candidates are initially rejected based on this criterion. The cut is increased in steps of 0.02cm whilst the remaining cuts are kept at their respective default values. After each cut has been implemented, the resulting K^0_S mass plot was generated and its significance was determined using a fitting function to obtain the signal and background levels. A plot of the significance of each mass plot against cut value was produced, shown in figure 1.

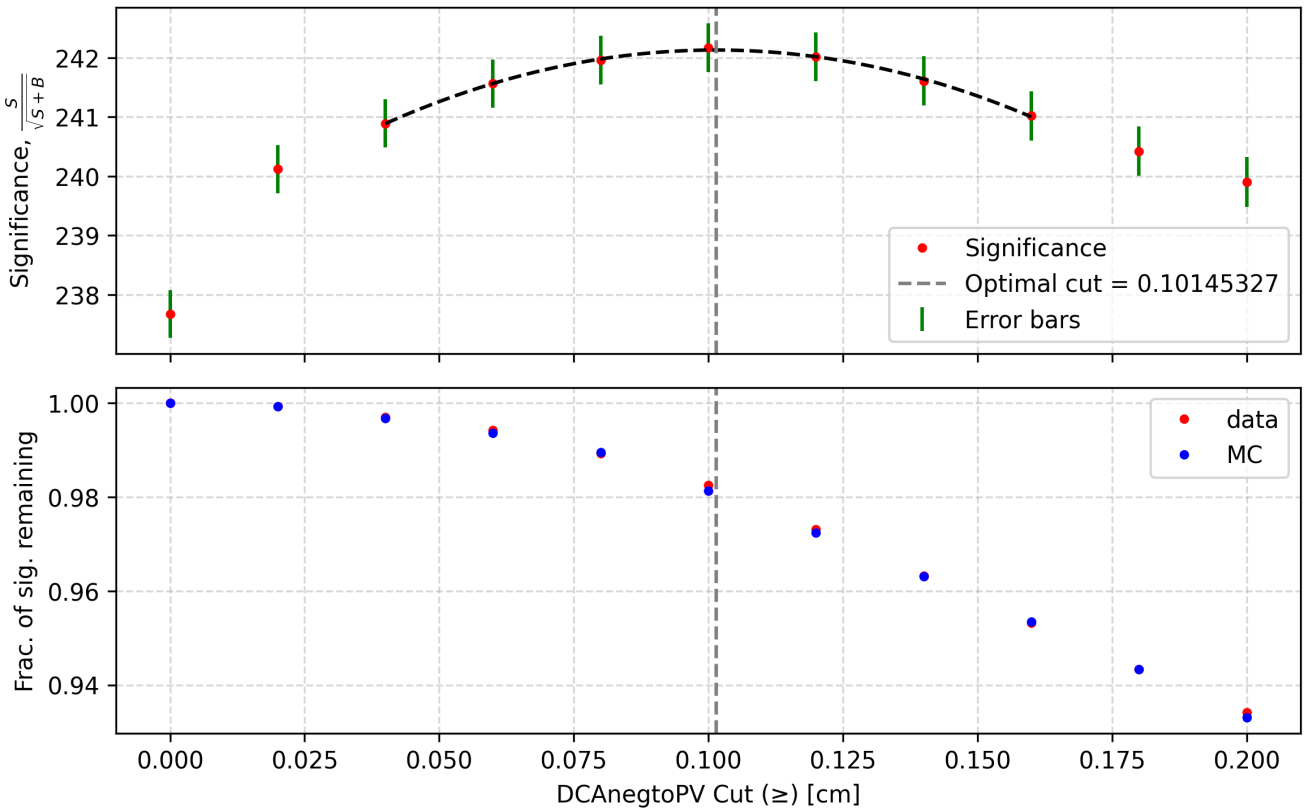

Figure 1: Significance of K^0_S mass plot and signal fraction remaining against DCAnegtoPV cut. The grey dotted line indicates the point at which significance was maximised.

In addition, the optimal cut must also occur at a point where the real data is accurately represented by the Monte Carlo (MC) data. To test this, each cut value was repeated for the MC data and the fractional signal loss for both channels was found by dividing the raw signal at each cut by the signal count at the default cut values. This results in a normalised value between 0 and 1, facilitating easy comparison between the real and MC data. This plot is also shown in figure 1, plotted beneath the significance plot against the same cut values. In this case, the cut value of >0.10145cm was selected since it maximised significance whilst also showing little discrepancy between the signal loss of the real and MC data. Notably, it also retained approximately 98% of the initial signal. Once all five selection cuts have been finalised an invariant mass plot of the particle may be obtained, in order to help verify the effectiveness of the cuts by observing the reduction in background.

3.2 Future Analysis

The following section outlines the future analysis to be undertaken by each partner during the remainder of this project, beginning with finalising the previously mentioned selection cuts. An approximate timeline of the results to be obtained is shown in figure 2.

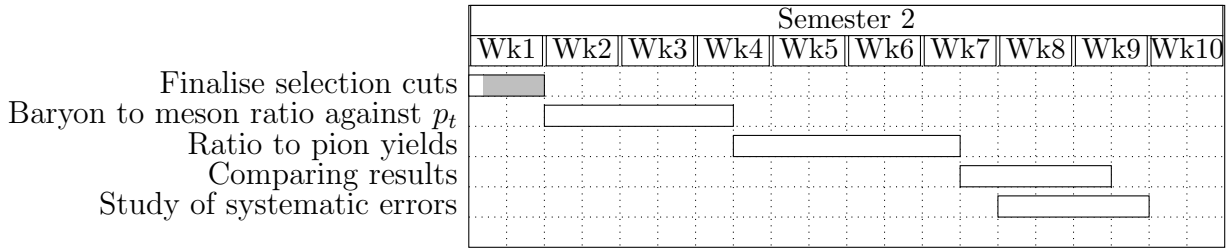

Figure 2: Gantt chart showing plan for remainder of project. Note that the seminar deadline is the end of week 8 and the final report deadline is the end of week 10.

A key result to be presented in the final report is the baryon to meson ratio, $\frac{\Lambda}{K_s^0}$, plotted as a function of transverse momentum, p_t. Examining this ratio at different transverse momenta may provide insights into the changing dynamics of Λ and K_S^0 production during the collision process[12]. In addition, the ratio of V^0s to pions may be plotted against final state multiplicity. Since pions are the lightest meson, many are produced during collisions, and they scale with the total number of particles produced. Hence, by normalising the yields of strange particles to the number of pions, any deviation from a flat line could serve as an indicator of strangeness enhancement. Such enhancement, characterised by an excess production of strange quarks and hadrons, is linked to the conditions of QGP[13]. Therefore, variations in this ratio offer a means to test the hypothesis that heavier collisions, associated with higher multiplicities, are more likely to create conditions conducive to QGP formation.

Such analytical approaches align with established methodologies in experimental heavy-ion physics and as such may be compared with similar analysis on previous runs, such as ALICE Run 2. Comparisons may also be made between each partner's analysis, to improve the reliability of the results, and to theoretical models, to test whether the data behaved as expected. Finally, the project will conclude with a systematic study of errors, which may include experimental uncertainties, modelling discrepancies and cross checks for consistency.

References

[1] P. Z. Skands (2014) Introduction to QCD https://arxiv.org/pdf/1207.2389v4.pdf

[2] Potter, T. (n.d.). Particle and Nuclear Physics: Lecture 07 - Quantum Chromodynamics (QCD). https://www.hep.phy.cam.ac.uk/~chpotter/particleandnuclearphysics/Lecture_07_QCD.pdf

[3] Quantum Diaries (2011, November 23). What is the QGP? https://www.quantumdiaries.org/2011/11/23/what-is-the-qgp/

[4] Johann Rafelski and Jeremiah Birrell 2014 J. Phys.: Conf. Ser. 509 012014

[5] CERN Document Server. ALICE Detector Schematic as during RUN3 (after upgrade) ALICE-PHO-SKE-2017-001-5 https://cds.cern.ch/record/2263642

[6] E. Daw (2012) Lecture 7 - Rapidity and Pseudorapidity https://www.hep.shef.ac.uk/edaw/PHY206/Site/2012_course_files/phy206rlec7.pdf

[7] I. Ravasenga. (2017). The upgrade of the Inner Tracking System of the ALICE experiment https://cds.cern.ch/record/2659644/files/fulltext.pdf

[8] Colella, D. (2020). ALICE ITS Upgrade for Run 3 Report for the ALICE collaboration https://cds.cern.ch/record/2746554/files/document.pdf

[9] Contin, G. (for the ALICE Collaboration). (2020). The MAPS-based ITS Upgrade for ALICE. arXiv:2001.03042 [physics.ins-det]. https://arxiv.org/abs/2001.03042

[10] CERN webpage (n.d.). ALICE TPC Gas System. https://alice-tpc.web.cern.ch/content/tpc-gas-system

[11] Weilin Yu (2013) Particle identification of the ALICE TPC via dE/dx https://www.sciencedirect.com/science/article/pii/S0168900212005098

[12] ALICE Collaboration (2020) Λ+c production and baryon-to-meson ratios in pp and p-Pb collisions at $\sqrt{s_{NN}}$=5.02 TeV at the LHC https://arxiv.org/abs/2011.06078

[13] Acharya, S., Adamová, D., Adhya, S.P. et al.(2020) Multiplicity dependence of (multi-)strange hadron production in proton-proton collisions at $\sqrt{S}$ = 13 TeV. Eur. Phys. J. C 80, 167 . https://link.springer.com/article/10.1140/epjc/s10052-020-7673-8